

The ABTS-HRP System as an Alternative Method to RRDE for the Determination of the Selectivity of the Oxygen Reduction Reaction

Xi Cheng^{1,4}, Lilyan Challier³, Arnaud Etcheberry², Vincent Noël³, Henri Perez^{1,*}

¹ Laboratoire Francis Perrin, CEA/DSM/IRAMIS/SPAM-LFP CNRS URA 2453 bât. 522, 91191 Gif/Yvette, France

² Institut Lavoisier (ILV, UMR 8180 CNRS, Université de Versailles Saint Quentin, 45 Avenue des Etats-Unis, 78035 Versailles, France

³ Université Paris Diderot, ITODYS, UMR 70 86 CNRS, 15 rue Jean-Antoine de Baïf, 75205 Paris cedex 13, France

⁴ Agence de l'environnement et de la Maîtrise de l'Energie 20, avenue du Grésillé- BP 90406 49004 Angers Cedex 01 France

*E-mail: henri.perez@cea.fr.

Received: 3 May 2012 / Accepted: 7 June 2012 / Published: 1 July 2012

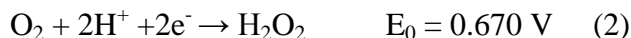
A 2,2'-azino-bis(3-ethylbenzothiazoline-6-sulfonate) (ABTS)-H₂O₂-peroxidase system was involved to study the oxygen reduction reaction (ORR) selectivity in acid medium. The average number of electron transferred per oxygen molecule (n) was calculated by measuring the quantity of H₂O₂ produced during the oxygen reduction reaction, taking advantage of the high activity of peroxidase enzyme coupled with the ABTS chromogen. The method was validated using electrode materials for which the electron pathway is established. It is simple, accurate and can be used on various kind of electrode structure.

Keywords: ORR, selectivity, hydrogen peroxide, porous electrodes

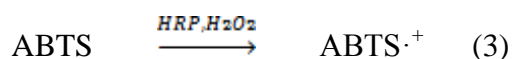
1. INTRODUCTION

Platinum based and as well as Non-noble Nanomaterials are extensively studied as electrocatalysts for the sluggish oxygen reduction reaction (ORR) in acid medium for proton exchange member fuel cell (PEMFC) [1-3]. An important issue in this field is related to the ORR selectivity *i.e.* the average number of electron transferred per oxygen molecule (n). Indeed, the oxygen reduction can

proceed by two major pathways: a “direct” four electron pathway (1) and a two electron “peroxide” pathway [4] (2).



The Rotating Ring Disk electrode is widely used to estimate the ORR selectivity, as it allows the amount of H_2O_2 produced during the reaction to be estimated. The measurement is performed on a sample of the electrocatalysts deposited on the disk. Due to the small area of the disk it is difficult to make a homogeneous deposit in term coverage and roughness. It is therefore of interest to develop alternative methods to RRDE measurement which can be applied to electrodes having various shape and feature. In this paper, the 2,2'-azino-bis(3-ethylbenzothiazoline-6-sulfonate) (ABTS)-peroxidase system [5,6] is used to measure the amount of H_2O_2 produced during the ORR. The measurement is based on the complete consumption of H_2O_2 by peroxidase in the presence of ABTS. ABTS regenerate peroxidase giving a radical-cation ($\text{ABTS}^{\cdot+}$) with an absorption maximum at 414 nm (3), the intensity of which is proportional to the amount of H_2O_2 initially present in the sample.



$$\lambda_{\text{max}} = 340 \text{ nm}$$

$$\lambda_{\text{max}} = 414 \text{ nm}$$

The determination of the H_2O_2 quantity produced was here obtained from calibration curves built using solutions containing ABTS-peroxidase couple and known amounts of H_2O_2 .

Chronoamperometry measurement was performed in O_2 saturated acid electrolyte on various electrodes, in order to measure the total number of mole of electron (MTe^-) consumed by oxygen reduction at a given time. At this time a volume of the electrolyte was submitted to H_2O_2 amount ($\text{M}_{\text{H}_2\text{O}_2}$) determination using ABTS-peroxidase mixture. The number of mole of electrons involved in the production of H_2O_2 ($\text{M}2\text{e}^-$) was calculated using equation (4), and the percentage of H_2O_2 ($\text{H}_2\text{O}_2\%$) was deduced from equation (5).

$$\text{M}2\text{e}^- = 2 \times \text{M}_{\text{H}_2\text{O}_2} \quad (4)$$

$$\text{H}_2\text{O}_2\% = \frac{\text{M}2\text{e}^-}{\text{MTe}^-} \times 100\% \quad (5)$$

Also, the average number of electron transferred per oxygen molecule (n) was obtained from equation (6)

$$n = 2 \times \text{H}_2\text{O}_2\% + 4 \times (1 - \text{H}_2\text{O}_2\%) \quad (6)$$

In order to check the feasibility of our method, n measurements were first carried out on electrode materials for which the ORR electron pathway is established. Bulk Pt was used as electrode material proceeding *via* the four electron pathway (1). Pure carbon nanotubes and chemically grafted carbon nanotubes with 2-aminoanthraquinone electrodes known as two electrons pathway ORR materials were used (2) [7-10]. Additional n determinations were finally performed on porous electrodes structures developed in our laboratory, which are based on organically capped platinum nanoparticle electrocatalyst (NP) and carbon nanotubes (CNT) [11,12].

2. EXPERIMENTAL PART

2.1 Chemicals

Horseshoe peroxidase (HRP RZ=3.2), 2,2'-azino-bis (3-ethylbenzthiazoline-6-sulfonic acid), diammonium salt (ABTS) and phosphate Buffered Saline (PBS), 2-aminoanthraquinone (AQ), NaNO_2 and HCl (37%) were purchased from Sigma Aldrich; H_2O_2 solution (30% v/v) and isopropanol were supplied by Merck; HClO_4 (70%) from Fluka.

2.2 Instrumentation

The electrochemical measurements were performed using Bio-Logic VMP3 potentiostat. The electrolyte was HClO_4 at the 0.1 M concentration. The counter electrode was a platinum foil and the reference electrode a Sodium-Saturated Calomel Electrode (SSCE, Radiometer Analytical). In the figures of the paper the potential has been reported vs. the Standard Hydrogen Electrode (SHE, -0.236 V vs. SSCE). UV-VIS spectra were recorded with a JASCO V-570 UV-VIS spectrophotometer. For calibration curves and H_2O_2 amount determination all the volumes were collected using Eppendorf micropipettes.

2.3 Electrodes

Bulk platinum electrode consisted in a 2 square centimeter foil and was used as 4 electron pathway ORR material. The multi-walled carbon nanotubes were produced by catalytic chemical vapor deposition as previously reported [13] and treated thermally (2000°C under argon), in order to remove the iron catalyst residue involved in the synthesis. Nanotubes were dispersed in isopropanol using a standard 12 liters ultrasound trough for 2 to 3 hours. Electrodes were formed as previously reported by filtration of a given volume of liquid dispersion on a carbon felt [11] (Freudenberg H2315 T10 A felts). These electrodes were used as formed (CNT electrodes) or were electrochemically grafted with 2-aminoanthraquinone (CNT-AQ electrodes), using the well established diazonium procedure (see S1). This gives electrodes able to reduce oxygen through the 2 electron pathway [8,9].

Electrodes based on organically capped platinum electrocatalyst and carbon nanotubes were formed using a two steps process extensively described elsewhere [11,12]. Briefly, a liquid

nanocomposite dispersion combining capped electrocatalyst and carbon nanotubes is prepared, in which the platinum density at carbon nanotube surface is well controlled and closely related to the mass ratio NP/CNT involved in the experiment. The active layers are then formed by vacuum assisted filtration of the nanocomposites liquid dispersion onto a carbon felt. The macroscopic geometrical area of the porous active layer formed on the carbon felt is generally 2.54 cm^2 . The platinum loading in these electrodes can be controlled by both, the feature of the liquid dispersion by changing the mass ratio NP/CNT or using different volumes of liquid dispersion involved in the filtration on the carbon felt. Different types of electrodes were prepared from different nanocomposite liquid dispersions: NP/CNT masse ratio 20% to give electrodes with a Pt loading of $38.6 \mu\text{gPt.cm}^{-2}$. NP/CNT masse ratio 3% to give electrodes with Pt loadings of, 2.1, 4.3, 6.4, 12.8, 17.0 $\mu\text{gPt.cm}^{-2}$. NP/NT mass ratio 10% to form electrodes having identical total amount of platinum but different platinum density of 19.3 $\mu\text{gPt.cm}^{-2}$ and 64.1 $\mu\text{gPt.cm}^{-2}$.

2.4 Spectrophotometric assay of H_2O_2

The solutions for the determination of the calibration curve and for H_2O_2 assay were prepared as:

1. HClO_4 0.1 M
2. H_2O_2 0.02 mM in HClO_4 0.1 M
3. PBS 1 tablet in 200 ml water, pH=7.4
4. A solution containing HRP (0.021 mg.ml^{-1}) and ABTS (0.0144 mM) prepared from PBS solution 3.

The spectrophotometric calibration was performed as follow: 3 ml of the solution HRP-ABTS-PBS and a given volume (for example $10 \mu\text{l}$) of H_2O_2 in HClO_4 0.1 M (solution 2) was added in the sample cuvette (Hellma 100-QX). Then 3 ml of the solution HRP-ABTS-PBS and $10 \mu\text{l}$ of HClO_4 0.1 M (solution 1) corresponding to the same H_2O_2 solution volume introduced in the sample cuvette, were added in the reference cuvette. The addition of HClO_4 0.1 M in the reference cuvette was performed to keep the same concentration of HRP and ABTS and to record the modification only induced by H_2O_2 . A scan between 200 nm and 800 nm was recorded right after the filling of the sample and reference cuvettes. The procedure was repeated for 30, 50, 70, 100, 200, 300 μl additions of H_2O_2 (solution 2) in the sample cuvette, and the same volumes of HClO_4 0.1 M (solution 1) in the reference cuvettes to establish the calibration curve. The high activity of HRP ensures a fast consumption of H_2O_2 . But the absorption which is recorded is due to the ABTS which regenerate the HRP. Thus, in order to make sure that the H_2O_2 added in the sample cuvette was consumed completely and rapidly, we set the concentration of ABTS in the cuvette much higher than that of H_2O_2 ($C_{\text{ABTS}} \geq 10C_{\text{H}_2\text{O}_2}$). All the measurements were carried out at room temperature. With $10 \mu\text{l}$ of addition, the concentration of

H_2O_2 is 6.10^{-8} M in the cuvette what is considered as the detection limit of the system in our experimental conditions. Also related to our experimental conditions the pH of the solution changes in the cuvette if more than 300 μl of HClO_4 (solution 1) is added, making HRP losing its catalyst activity [14].

2.5 Electrochemistry

Electrodes that incorporate carbon nanotubes are porous and were impregnated by the electrolyte using a reported procedure [11]. First, for each kind of electrodes, cyclic voltammetry was performed in O_2 and Argon saturated electrolyte at 100 mV/s, to clearly identify the reduction peak related to oxygen reduction. These peak potentials values (vs. SHE: 0.5 V for Bulk Pt, -0.025 V for CNT electrode, -0.4V for CNT-AQ electrode) were used to perform the chronoamperometry. During the measurement the electrolyte was kept under mechanical magnetic stirring and permanent bubbling of O_2 . Then, determined volumes of the electrolyte were collected and were introduced in the quartz cell (see above) for spectrophotometric detection and assay of H_2O_2 possibly produced during the ORR.

3. RESULTS AND DISCUSSION

3.1 Calibration curve for H_2O_2 assay

Figure 1 shows the UV-Visible spectra recorded on sample cuvettes right after the addition of increasing amount of H_2O_2 .

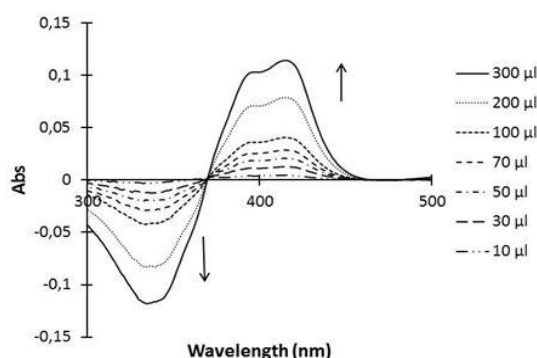


Figure 1. Absorption spectrum of the solution containing HRP ($0.021 \text{ mg}\cdot\text{ml}^{-1}$) and ABTS (0.0144 mM) in PBS ($\text{pH}=7.4$) with different addition volume of H_2O_2 (solution 2).

It is seen that the $\text{ABTS}^{\cdot+}$ radical specific absorption peak at 414 nm [5,6] increases with the H_2O_2 concentration. Concomitantly, a negative absorption appears at 340 nm which is the maximum absorption wavelength for ABTS [5,6]: indeed, initially the sample and reference cuvettes contain

ABTS at the same concentration, but the addition of H₂O₂ in the sample cuvette results in the ABTS consumption. This leads to a decrease of ABTS concentration in the sample cuvette producing a negative absorption on the spectra, the intensity of which is directly related to the absorption of the ABTS^{•+} radical which is formed from ABTS. Presumably due to the “back” reaction of ABTS^{•+} into ABTS [6], a time-dependent decay of the absorption at 414 nm absorption was observed (Figure 2). This indicates that the UV-VIS measurements must be carried out within quite after the addition of the H₂O₂ into the cuvette. A linear calibration curve was obtained by plotting the absorbance of ABTS^{•+} according to the concentration of hydrogen peroxide, giving quite reproducible slopes (Figure 3a). An average value of 61347 was calculated over fourteen calibration curves, with a maximum variation of ± 3.4 % (Figure 3b). Furthermore, we found that HRP-ABTS in PBS (solution 4) and H₂O₂ in HClO₄ (solution 2) that serve for building the calibration curve could be stored at 6°C at least for a week and produce quite similar the calibration curves: slope changed from 60358 to 62013 (see supporting info S2).

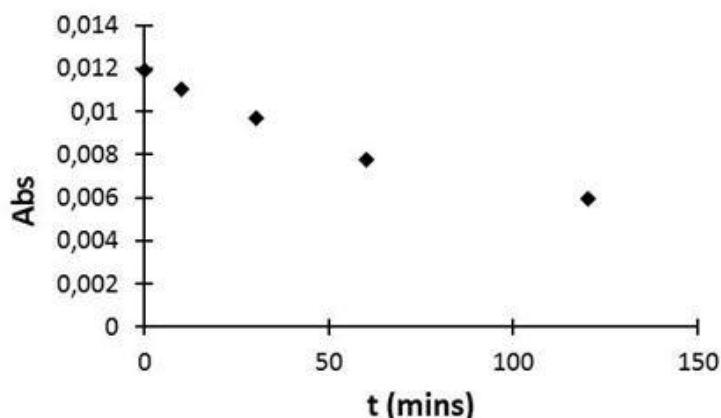
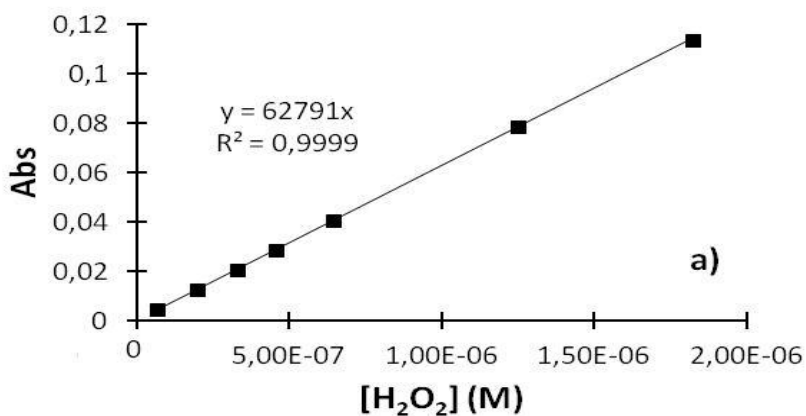


Figure 2. The variation of Absorbance against time after the addition of 30 µl of H₂O₂ (solution 2) in 3 ml of the solution containing HRP (0.021 mg.ml⁻¹) and ABTS (0.0144 mM) in PBS (pH=7.4)



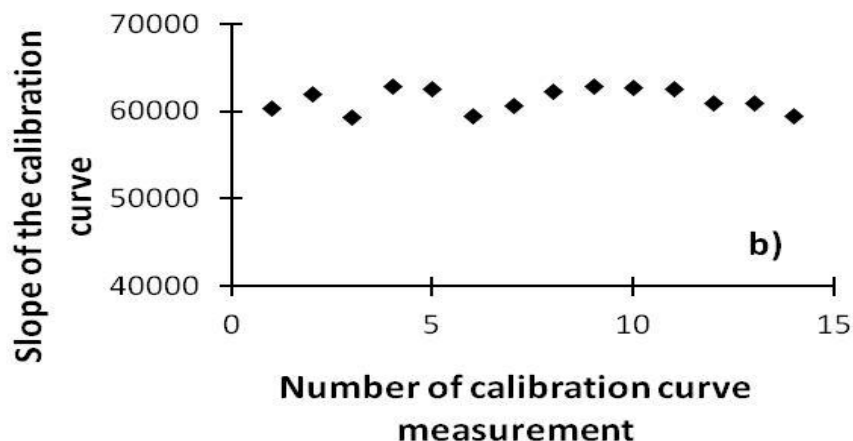


Figure 3: a) Calibration curve representing the variation of Absorbance against concentration of hydrogen peroxide b) Slopes for fourteen calibration curves.

3.2 Selectivity measurement by H₂O₂ assay on 4 and 2 electron ORR pathway materials

Figure 4 shows the integral of the chronoamperometry data as a function of time for 4 and 2 electrons ORR pathway electrodes: the bulk platinum, the CNT electrode and the CNT-AQ electrode.

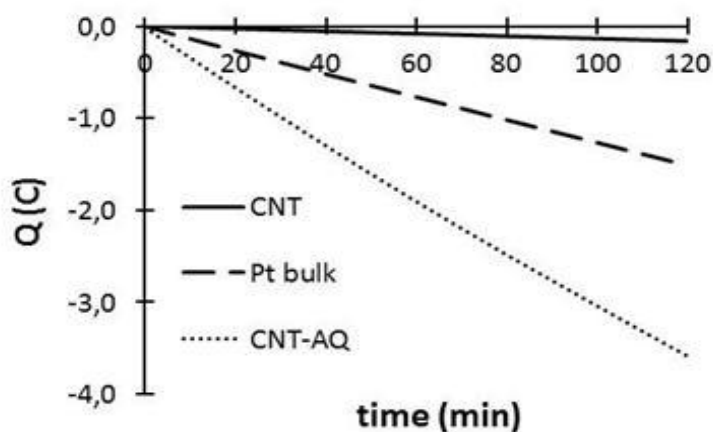


Figure 4. Integral of the current of chronoamperogrammes for bulk Pt, CNT and CNT-AQ electrodes.

Every 30, 60 and at a maximum of 120 minutes a given volume of the electrolyte was collected for the different electrodes studied and submitted to spectrophotometric measurement for H₂O₂ amount determination. Figure 5 reports examples of UV-Visible spectra showing: for the Pt bulk electrode the absence of H₂O₂ even after 2 hours ORR duration, and the production of H₂O₂ for the CNT and CNT-AQ electrodes after 30 minutes.

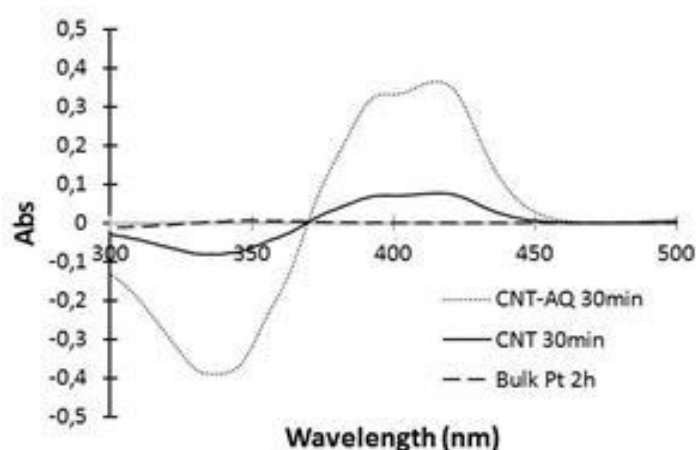


Figure 5. Absorption spectrum of the solution containing HRP ($0.021 \text{ mg}\cdot\text{ml}^{-1}$) and ABTS (0.0144 mM) in PBS ($\text{pH}=7.4$) with $300 \mu\text{l}$ addition of the electrolyte for the electrodes CNT and CNT-AQ after 30 min of chronoamperometry measurement; and bulk Pt electrode after 2 h of chronoamperometry measurement. As mentioned in the case of figure 1 (see the text), the negative absorption at 340 nm is due to the decrease of ABTS concentration in the sample cell which is related to H_2O_2 consumption.

At the same time when the electrolyte was collected, the charge (Q_{ORR}) corresponding to the ORR was noted and the number of mole of electron (MTe^-) was calculated (equation 7). From the total number of mole of H_2O_2 produced, the number of mole of electron corresponding to the $2e^-$ pathway was calculated (equation 4) as well as the percentage of H_2O_2 produced by oxygen molecule consumed (equation 5). The average number of electron transferred per oxygen molecule (n) can be obtained from (equation 6)

$$\text{MTe}^- = Q_{\text{ORR}}/F \quad (7)$$

Figure 6 shows the average number of electron transferred per oxygen molecule (n) consumed as a function of the assay time. The percentage of H_2O_2 produced at each given time for each sample is also reported. It is clearly seen that the bulk platinum electrode gave the expected 4 electron ORR reduction pathway, whatever the assay time. For CNT and CNT-AQ electrodes the expected 2 electron ORR pathway was found, but n becomes slightly higher than 2 when the assay time was higher than 30 minutes. We found that this is due to both stirring and oxygen bubbling and H_2O_2 disproportionation which induce a loss of H_2O_2 . This has been shown by dedicated studies of H_2O_2 concentration stability in the electrolyte as a function of time. It is worth to note that corrected values for n can be calculated for assay time higher than 30 minutes (see supporting information S3). According to these results, we propose 30 minutes as the duration of the chronoamperometry measurement, so we do not have to correct the value of n what makes the method more practical.

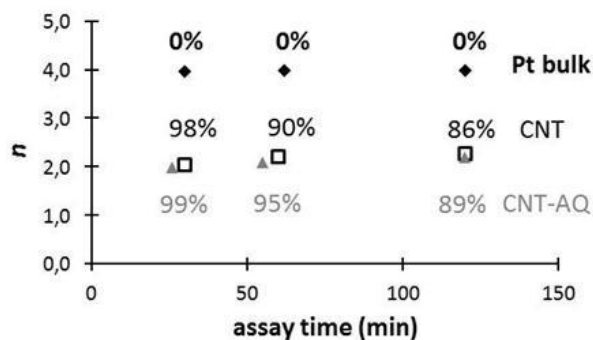


Figure 6. The number of electrons transferred per Oxygen molecule (n) and the percentage of H_2O_2 produced as a function of the time of chronoamperometry for Bulk Pt, CNT and CNT-AQ electrodes.

3.3 ORR Selectivity measurements on porous electrodes based on carbon nanotubes and organically capped platinum electrocatalyst.

Figure 7 shows a macroscopic view of the electrode as well as a transmission electron microscopy image of the capped-Pt/CNT electrocatalyst in which the Pt nanoparticles are clearly observed at the CNT surface. The experiments were performed as presented above for the determination of n . First, Porous electrodes in which the mass ratio Pt/CNT was set at 20 % (Pt/CNT 20%) and the total Pt loading was $98.0 \mu\text{g}$ ($38.6 \mu\text{gPt}\cdot\text{cm}^{-2}$) were studied as well as electrodes in which the mass ratio Pt/CNT was 3% (Pt/CNT 3%). For the latter different volumes of liquid dispersion were used to give electrodes with a total Pt loading of 5.4, 10.8, 16.2, 32.4 and $53.5 \mu\text{g}$. Through these experiments our goal was first to show that the method presented in this paper to determine ORR selectivity can be used even on such original electrode structures.

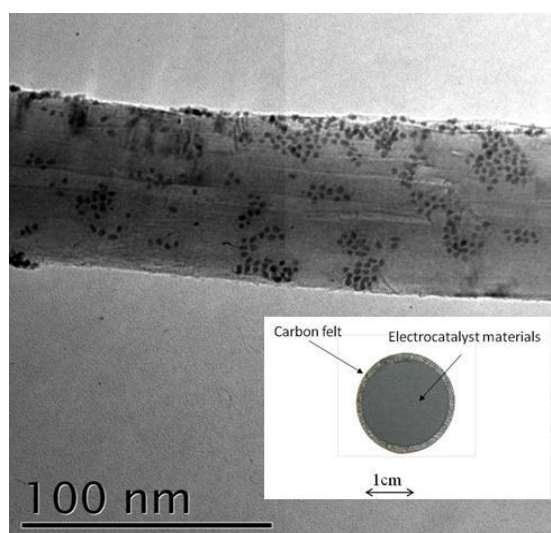


Figure 7. Transmission electron microscopy of capped-Pt on CNT. The insert show a macroscopic view of the electrode.

Second, experiments were performed to get preliminary results regarding the selectivity changes as a function of parameters such as the potential at which the ORR is performed, or the platinum loading in the electrode. Results related to the first point are shown in figure 8, in the same way as in figure 6, *i.e.* with the value of n and the percentage of H_2O_2 produced as a function of time. For the Pt/CNT 20 % electrode it is seen that at 0.5 V vs. SHE n is very close to 4 (3.99) and that the percentage of H_2O_2 produced is between 0.35 and 0.45 %. When the potential is lowered by 0.1 V n is slightly lower (3.92) and the percentage of H_2O_2 increase by a factor close to ten.

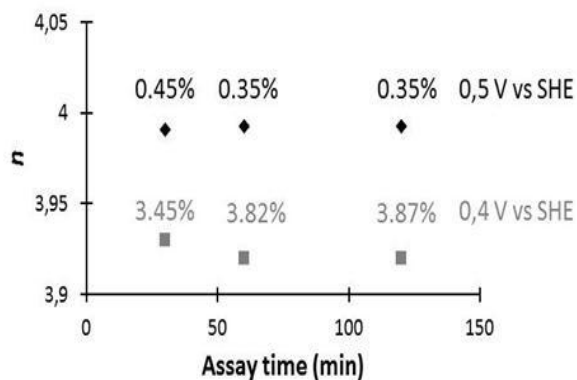


Figure 8. The number of electrons transferred per Oxygen molecule (n) and the percentage of H_2O_2 produced as a function of the time for chronoamperometry recorded on Pt/CNT 20% at 0.5 V vs. SHE and Pt/CNT 20% at 0.4 V vs. SHE.

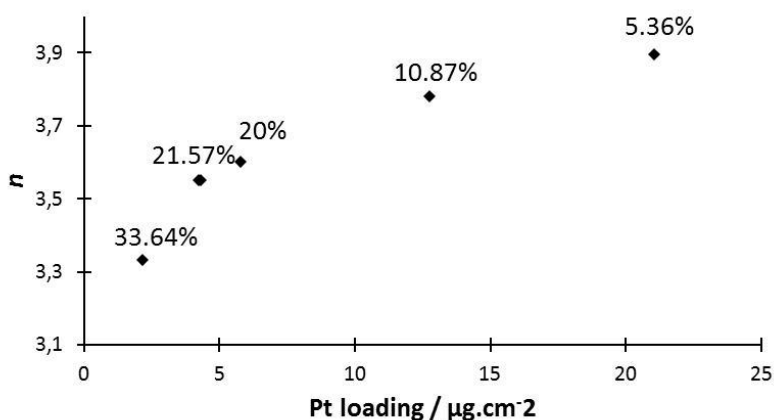


Figure 9. The number of electrons transferred per Oxygen molecule (n) and the percentage of H_2O_2 produced as a function of Pt loading ($\mu\text{g}/\text{cm}^2$) for Pt/CNT 3% electrodes (assay time 30min).

Figure 9 shows the determination of n for different Pt/CNT 3% electrodes in which the platinum loading is increased by increasing the amount of material deposited by filtration on the carbon felt. It is seen that n increases as a function of the platinum loading and tends to level off for the highest loadings. The trends we observe here which are first, an influence of the potential on the selectivity of the ORR (figure 8), and second a modification of the recorded selectivity as a function of the electrocatalyst loading (figure 9) are similar to those reported in the literature using RRDE

measurements for platinum based as well as non noble electrocatalyst materials¹⁵⁻¹⁷. A strong advantage of our method is that it can be implemented directly on “real” porous electrode structures. In order to illustrate this point a last set of experiment was performed using Pt/NT 10% composite liquid dispersion as follows: 60 ml of the later were used to prepare two different electrodes using 30 ml for each one. The first electrode had a macroscopic active layer area of 2.54 cm² and the second one (prepared using the same filtration device but using a mask to reduce the area of the active layer) had an area of 0.78 cm². Therefore the catalyst composite structure is the same for both electrodes, the total amount of platinum is also the same ($\approx 50 \mu\text{gPt}$) but the platinum density is 19.3 $\mu\text{gPt}\cdot\text{cm}^{-2}$ for the first electrode and 64.1 $\mu\text{gPt}\cdot\text{cm}^{-2}$ for the second one. The results for n are shown in figure 10, definitely indicating that the crucial parameter for selectivity is the electrocatalyst density.

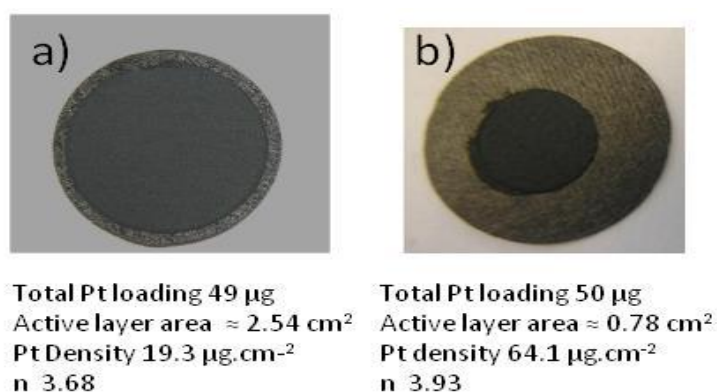


Figure 10. Electrode prepared using the same NP/NT 10% mass ratio liquid dispersion, having the same total amount of Pt but different platinum density.

Finally, additional experiments were performed on Pt/CNT electrodes to check a possible effect of H₂O₂ heterogeneous disproportionation that could disturb the selectivity measurement (see supporting information S4). We found that the influence of the disproportionation of H₂O₂ on our measurements is negligible and our data suggest that disproportionation is related to the total amount of platinum rather than platinum density.

4. CONCLUSION

In this paper we reported an alternative method to the RRDE for the determination of the ORR selectivity. It has been validated using well known electrode materials for which the expected ORR selectivity is recorded. The method is simple, quite accurate and can be used whatever the feature of the electrode (shape, bulk, porous). Preliminary results on the ORR selectivity obtained on porous electrodes based on organically capped platinum electrocatalyst and carbon nanotubes as a function of various parameters (Pt loading, effect of potential on H₂O₂ production) have been recorded. The trends are consistent with those reported using RRDE for Pt electrocatalyst and non-noble electrocatalyst. Coming reports will involve the systematical study of the ORR selectivity using the present method on electrodes based various nanomaterial electrocatalysts.

ACKNOWLEDGMENTS

This work was supported by the following French agencies: Agence de l'Environnement et de la Maîtrise de l'Energie (ADEME) and Agence National de la Recherche (ANR) through its HPAC-2009 program (project "Facteur 10").

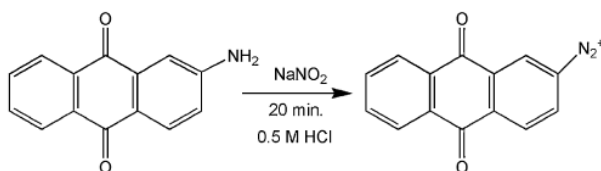
References

1. N.M. Markovic, P.N. Ross Jr., *Surf. Sci. Rep.* 45 (2002) 117.
2. F. Jaouen, J. Herranz, M. Lefèvre, J-P. Dodelet, U.I Kramm, I. Herrmann, P. Bogdanoff, J. Maruyama, T. Nagaoka,; A. Garsuch,; J. R. Dahn, T. Olson, S. Pylypenko, P. Atanassov, E.A. Ustinov, *ACS Applied Materials interfaces*, 2009, 1, 8, 1623-1639
3. *Electrocatalysis, Frontiers in Electrochemistry*, Vol. 5, J. Lipkowski and P. N.Ross, Jr., Editors, VCH, New York (1997)
4. E. Yeager, *Electrochim.Acta*, 1984, 29, 1527-1537
5. R. E.Childs, W. G. Bardsley, *Biochem. J.* 1975 145, 93-103
6. E.N. Kadnikova, N.M. Kostic, *Journal of Molecular Catalysis B : Enzymatic*, 2002, 18, 39-48
7. M. Gara and R.G. Compton, *new J. Chem.* 2011, 10, 1039
8. M. Kullapere, J-M. Seinberg, U. Mäeorg, G. Maia, G.; D. J. Schiffrin, K. Tammeveski, *Electrochim. Acta* 2009, 54, 1961-1969
9. B. Sljukic, C. E. Banks, R. G. Compton, *Iran J. Chem. Soc.* 2005, 2, 1
10. *Comprehensive Treatise of Electrochemistry, Vol 7: Kinetics and Mechanisms of Electrode Processes*, ed. B. Conway, J. Bockris, E. Yeager, S. Khan, R. White, Plenum Press, New York, 1983, vol. 7, pp. 301-398
11. B. Baret, P-H. Aubert, M. Mayne-L'Hermite, M. Pinault, C. Reynaud, A. Etcheberry, H. Perez, *Electrochim. Acta.* 2009, 54, 5421
12. G. March, F. Volatron, F. Lachaud, X. Cheng, B. Baret, M. Pinault, A. Etcheberry, H. Perez, *Electrochim. Acta.* 2011, 56, 5151-5157
13. M. Pinault, V. Pichot, H. Khodja, P. Launois, C. Reynaud, M. Mayne-L'Hermite, *Nano Lett.* 2005, 5, 12, 2394
14. O. V. Ignatenko, I.G. Gazaryan, E.A. Mareeva, *Biochem. J.* 2000, 65, 583-587
15. N. Alonso-Vante, N. *ChemPhysChem.* 2010, 11, 13
16. E.J. Biddinger, D. Von Deak, D. Singh, H. Marsh, B. Tan, D.S. Knapke, U.S. Ozkan, *J. Electrochem. Soc.* 2011, 158, B402-B409
17. A. Bonakdarpour, M. Lefevre, R.Z. Yang, F. Jaouen, T. Dahn, J-P. Dodelet, *J Electrochem. and Solid-State Lett.* 2008, 11 (6), B105-B108

SUPPORTING INFORMATION:

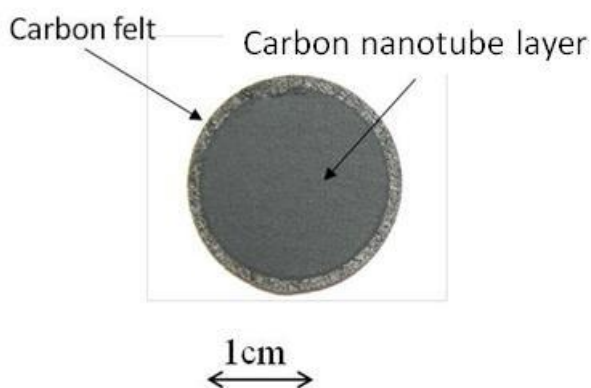
S1: Preparation of the CNT-Aminoanthraquinone electrode

The electrochemically assisted grafting of the CNT surface was performed with *in situ* generated AQ diazonium cations (scheme 1) in aqueous acidic electrolyte (HCl 0.5 M). First, a 0.5 M HCl solution containing 2 mM of 2-aminoanthraquinone and 4 mM NaNO₂ was prepared,



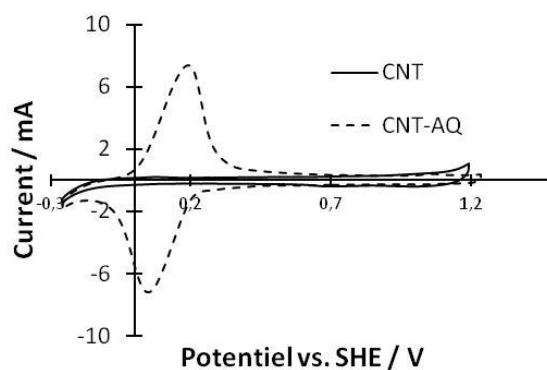
Scheme 1 : Diazotization of 2-aminoanthraquinone with NaNO_2 in 0.5 M HCl

Second, a CNT electrode was formed by filtration of a given volume of dispersion of CNT in isopropanol on a carbon felt (Scheme 2), then the CNT electrode was immersed in 30ml of 0.5 M HCl electrolyte with 3ml of the AQ diazonium solution in 0.5 M HCl.



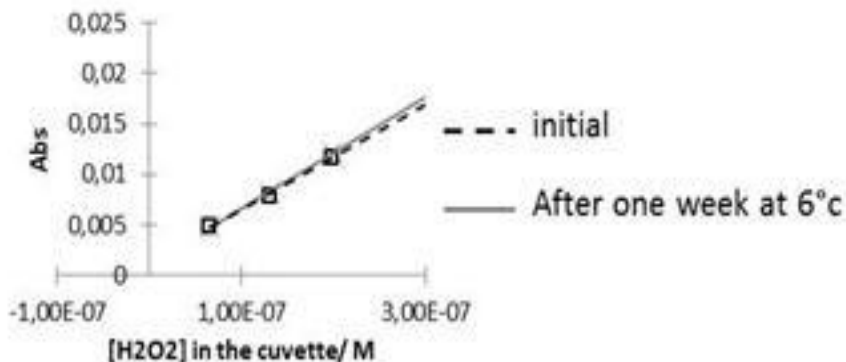
Scheme 2: porous electrode based on carbon nanotubes prepared by filtration on a carbon felt

Cyclic voltammetry was performed between 1.2 and -0.25 V vs. SHE at a sweep rate (v) of 100mVs^{-1} in argon saturated condition to perform the electrochemically assisted grafting at the carbon nanotube surface. The grafted CNT layer was then separated from the carbon felt by sonication of the electrode in isopropanol for 5 min. A filtration of the AQ-grafted CNT was performed on a new carbon felt. This process was repeated twice to remove any possibly ungrafted AQ. The combination of AQ with CNT was evidenced by cyclic voltammetry (HClO_4 1M) on which the redox peak of AQ were clearly observed (see below).



S2: H_2O_2 assay Calibration curves drawn from an HPR-ABS solution after one week storage at 6°C

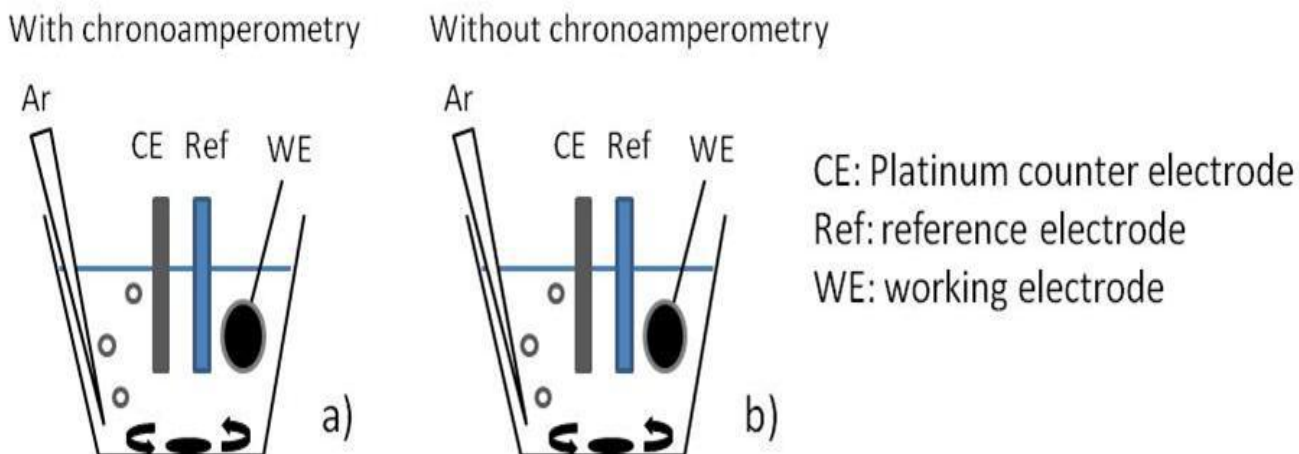
The curves are unchanged indicating the stability of the HRP-ABTS solution used for the H₂O₂ assay.



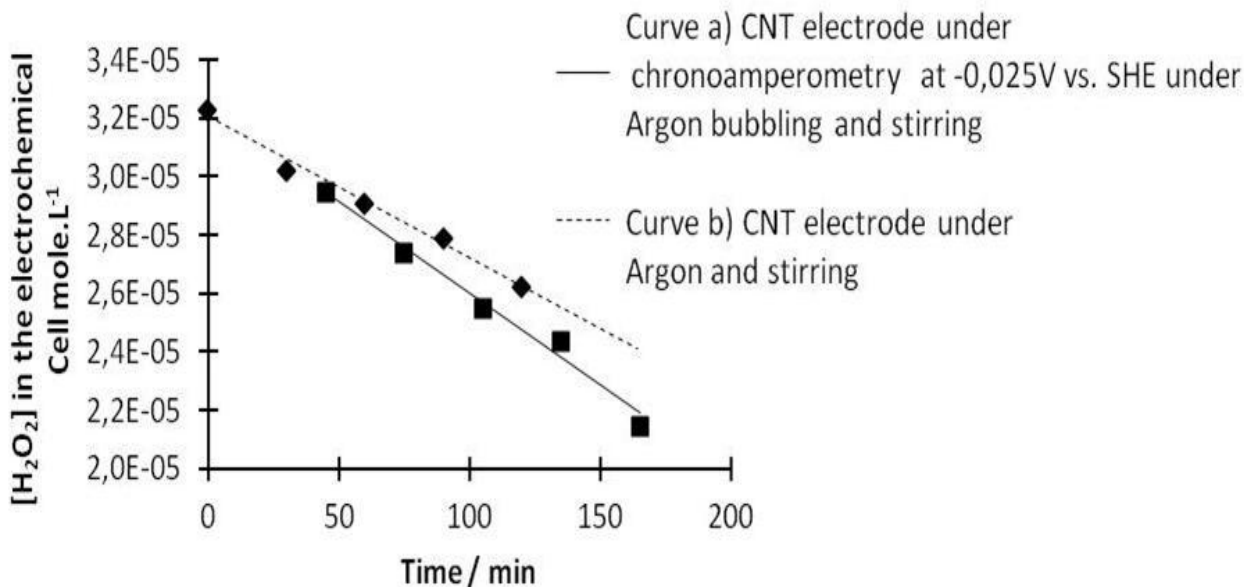
S3: Additional experiments aiming at the understanding of the decrease of *n* as a function of assay time for data related to 2 electron pathway electrode materials

These experiments were performed in order to get insights in the reasons for which the average number of electron determined using our method tends to increase with time when 2 electrons pathway electrodes were studied (figure 6 in the paper).

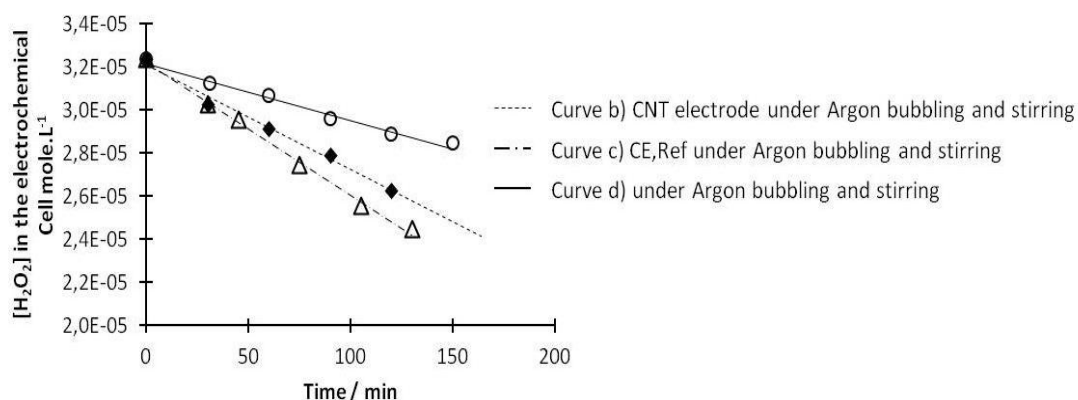
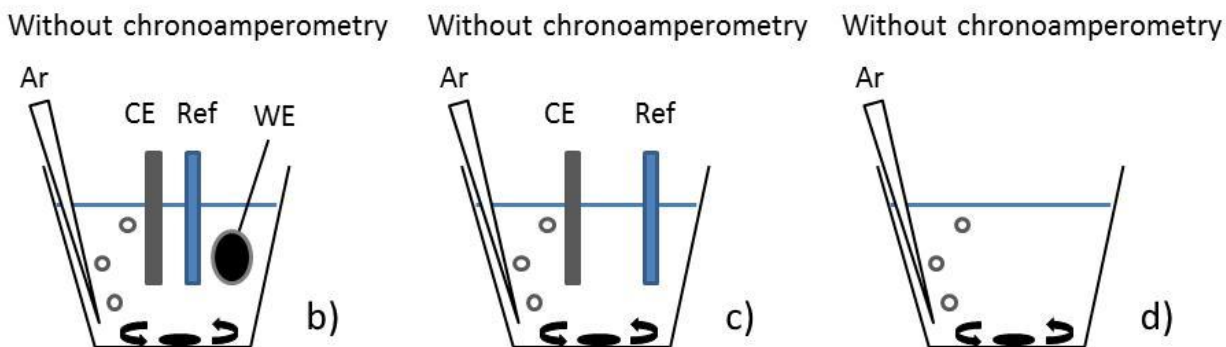
The increase observed for *n* as a function of the assay could be related to a decrease of H₂O₂ concentration in the electrolyte with time. The later point can be due to i) the electrochemical consumption of H₂O₂, and/or ii) the disproportionation (homogenous or heterogenous) of H₂O₂. To check these points the electrochemical cell was filled with 30 ml HClO₄ 0.1M and an adapted amount of H₂O₂ was added in order to obtain a concentration close to 3.2 10⁻⁵ M. Then the following experiments were performed:



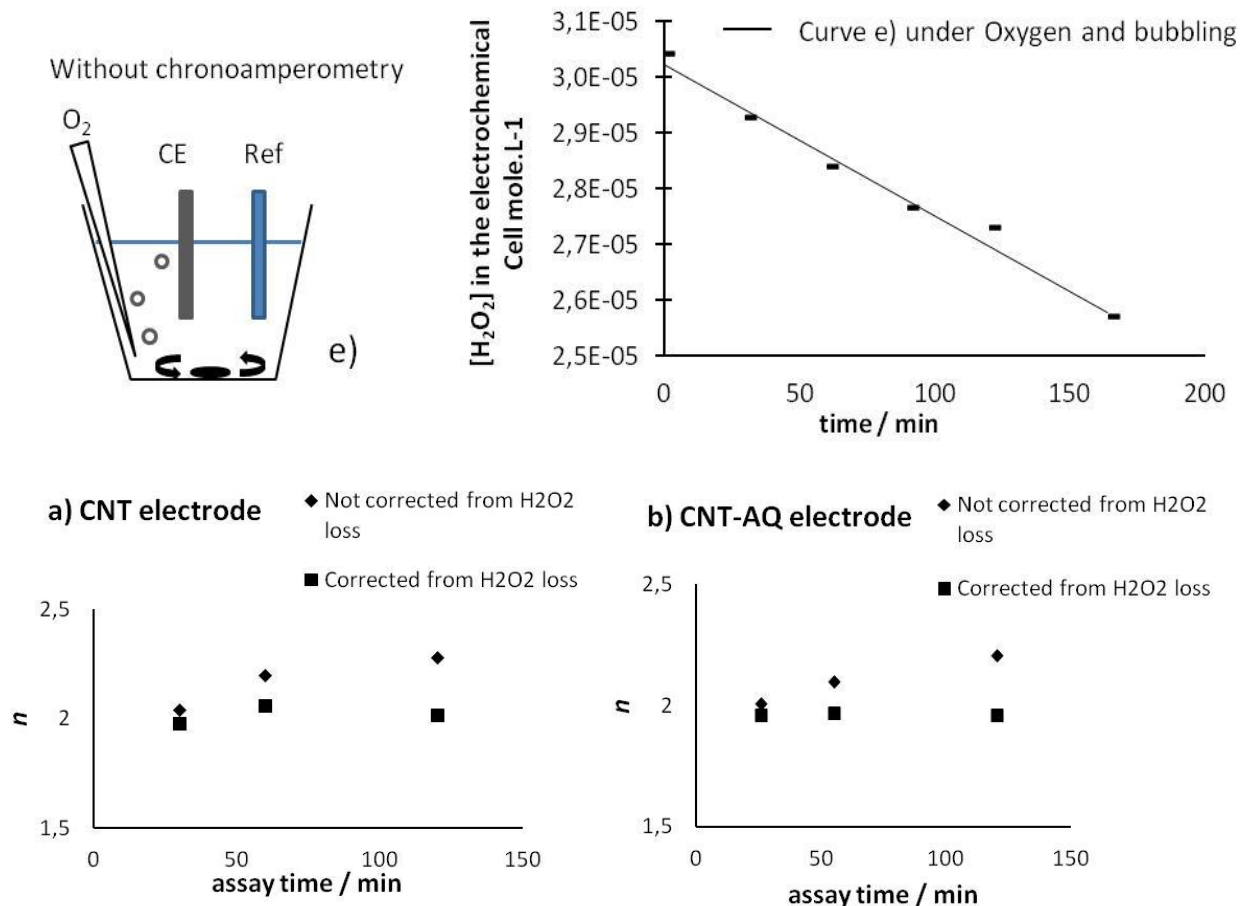
To address (i) two experiments were performed in which the electrolyte was continuously bubbled with argon and kept under stirring. In the first one a carbon nanotube based porous electrode (working electrode WE) was submitted to chronoamperometry and H₂O₂ concentration was monitored as a function of time (scheme a, curve a): It was found (curve a) that the amount of H₂O₂ decreased with time. The second experiment (scheme b, curve b) consisted in the same as the first one but without chronoamperometry. Identical trends for H₂O₂ concentration were observed in both experiments (see below) thus indicating that the decrease on the H₂O₂ concentration is not induced by the electrochemistry.



To address (ii) two additional experiments were performed consisting in H_2O_2 concentration monitoring as a function of time under argon bubbling and mechanical stirring: in the first one (scheme c, curve c) only the platinum counter electrode used for chronoamperometry was immersed in the electrolyte in the second one the electrolyte only was in the cell (scheme d, curve d). Curves b) and c) revealed the same trends while curve d) showed a lower decrease for the H_2O_2 concentration. Therefore it is concluded that the loss of H_2O_2 is due in part to H_2O_2 disproportionation on platinum counter electrode (CE) and to a lesser extent to argon bubbling and stirring (may be reflecting homogeneous disproportionation in such experimental conditions)



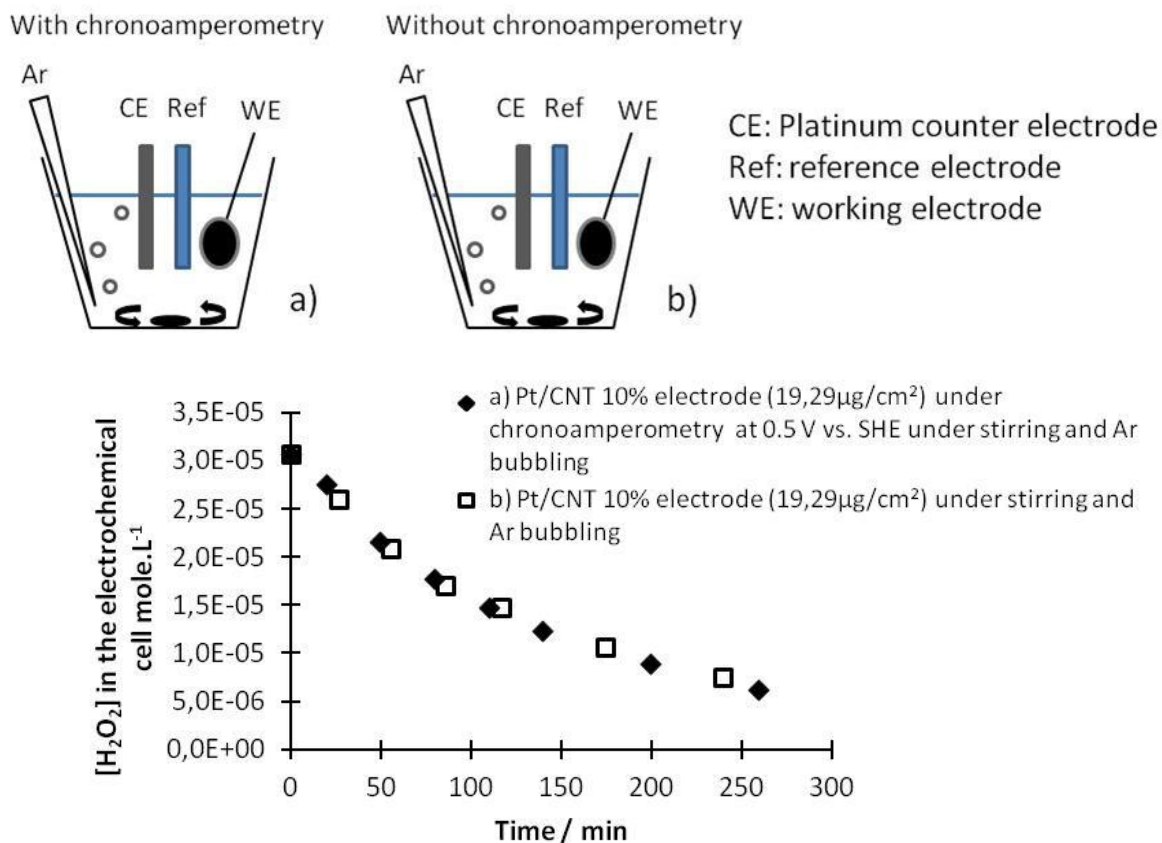
Finally because the selectivity determination is performed under O₂ bubbling and continuous stirring a last experiment was performed (scheme e, curve e), in which H₂O₂ concentration was monitored as a function of time in such conditions. The data from curve e) were used to correct the value of *n* as shown below for CNT and CNT-AQ electrodes.



S4: Checking the impact of heterogeneous H₂O₂ disproportionation for Pt/NT based porous electrodes.

Because the H₂O₂ concentration in the electrolyte may vary due to heterogeneous disproportionation when Pt loaded electrodes are involved the amount of H₂O₂ measured could be underestimated. Therefore, experiments reported below were performed in order to evaluate possible need for the correction of *n* due to the loss of the H₂O₂.

First, two electrochemical cells were filled with 30 ml HClO₄ 0.1M under continuous argon bubbling and mechanical stirring and an adapted amount of H₂O₂ was added in order to obtain a concentration close to 3.0 10⁻⁵ M. In the first cell a Pt/CNT 10% electrode (19.29μg.cm⁻²) was connected to the potentiostat and submitted to chronoamperometry at 0.5 V vs SHE. The H₂O₂ concentration was monitored as a function of time (scheme a, curve a). In the second cell the same experiment was conducted expect that no chronoamperometry was performed (scheme b, curve b)



The figure above shows that the decrease of H₂O₂ concentration over time is only due to the heterogeneous disproportionation of H₂O₂ and that there is no significant effect due to the polarization of the electrode on the H₂O₂ loss. Using the data shown in S4, we can correct the value of *n* for our Pt/CNT 10% electrode (19.3μg.cm⁻²), (this even if the loss is over estimated because we have seen that the H₂O₂ loss is lower under O₂ than Argon). It is found that this correction has negligible effect on the results, the value of *n* change from 3.68 to 3.64 after the correction.

In a third experiment the heterogeneous disproportionation was recorded for the two electrodes shown in figure 10 which were prepared using the same Pt/NT 10% liquid dispersion, and the same volume of the later (30mL). These electrodes had thus the same total platinum loading (≈ 50 μg.cm⁻²) but differ from each other by the macroscopic area of the active layer formed on the carbon felt and therefore differ by their platinum density (19.3μg.cm⁻² and 64.1 μg.cm⁻²). Scheme b and c picture these experiments in which the H₂O₂ was monitored over time. Curves b and c (see below) indicates that the H₂O₂ disproportionation was identical in both cases. Therefore the heterogeneous disproportionation of H₂O₂ does not depend on the platinum density in contrast to the value of *n* (see the paper).

